Proceedings of the 7th International Symposium on Cavitation
CAV2009 – Paper No. 143
August 17-22, 2009, Ann Arbor, Michigan, USA

Prediction of tip vortex cavitation inception on marine propellers at an early design stage

J. Hundemer
Hamburg University of Technology
Hamburg, Germany

M. Abdel-Maksoud
Hamburg University of Technology
Hamburg, Germany

ABSTRACT

The inception of vortex cavitation at an early design stage is still difficult to forecast. The most reliable prediction of the full scale performance is achieved by means of model tests, which are possible for few designs only. A simplified model to calculate the inception of tip vortex cavitation is developed and tested. The model is based on results obtained from potential flow theory, using a boundary element method. The developed tip vortex cavitation inception model and also the panel method are described, after a short introduction to vortex cavitation. The numerical behaviour of the model is investigated for an elliptic wing at different angles of attack and two marine propellers in homogenous and not axially symmetric inflow. The cavitation model's properties concerning different Reynolds numbers are studied and the scale effects on calculated model- and full-scale tip vortices are discussed.

INTRODUCTION

Potential flow based methods do still play an important role in propeller design. Though many effects due to viscosity are neglected, performance prediction for thrust and torque can be estimated with sufficient accuracy, especially at design conditions. Compared to field methods like RANSE- and LES-methods, which do account for viscosity in more detail, potential based methods are known for their computational efficiency, which makes them attractive to optimization based propeller design.

At early design stages of a propeller not only thrust and torque of possible propeller geometries are of interest. Also an accurate prediction of cavitation inception is an important key to develop a successful propeller design. Hence, many potential flow based propeller design methods contain a module to calculate the extension of sheet cavitation and some also are able to detect the risk of bubble cavitation. Only few theoretical work is published on the prediction of vortex cavitation inception on marine propellers on the basis of potential flow theory [11], [7], [8], some deal with developed vortex cavitation and its influence on other structures [11], [9]. This is probably due to the fact that vortex cavitation is still not fully understood, especially if scalability of model test results and gas content of the fluid are concerned [1]. Nevertheless there still is a demand for information about vortex cavitation inception at an early design stage in particular at high Reynolds numbers.

The paper gives a description of a new developed panel method, which includes a model for calculation of the pressure distribution in the tip vortex core and the beginning of vaporization in the core. The vorticity, which is shed into the flow at the trailing edge of the propeller blades to satisfy the Kutta condition, is related to the bound vorticity of the blades and moves with the free flow behind the propeller. These so called free vortices lead to a roll up and a formation of tip and hub vortices. It has been shown [9] that this process can be predicted quite well with potential flow based methods, similar to the panel method used here. The roll up is usually calculated in an iterative manner for stationary processes or alternatively tracked in unsteady simulations. By analysing the deformed panel geometry of the free vortices behind the propeller blades the increasing strength of the tip vortex is calculated. Hence, a radius of the roll up is determined and it is assumed that only the vorticity of all panels inside this radius contribute to the strength of the tip vortex.

In addition to the vortex strength, a model for the pressure distribution inside the vortex is needed. In the developed method the Hamel-Oseen [12] vortex model is applied. The model is based on an analytical solution of the Navier-Stokes-Equation. Compared to the Rankine vortex formulation, which was chosen by other authors [11], [8], the maximum pressure drop induced by the vortex is smaller and it is reported that the velocity distribution inside the vortex is more realistic. Both, the Rankine and Hamel-Oseen vortex assume a viscous vortex core with an initial diameter, which has to be predefined. Following the vortex formulation by Hamel and Oseen the vortex core grows with the age of the vortex, which leads to a decreasing pressure drop induced by the ageing vortex. According to [1], [10] the pressure minimum and thus the core diameter have to be scaled with Reynolds number, as the core

diameter can be related to the boundary layer thickness at the blade. The boundary layer, which is typically turbulent for full-scale propellers, can be estimated by some experimentally developed formula depending on the local Reynolds number at the tip of the blade. With the information about vortex strength and vortex core diameter the pressure drop inside the vortex is estimated and a cavitation inception number can be derived.

VORTEX CAVITATION

The development of vortices induced by the lift generation at a wing of finite length is a complex process, which can result in a cavitating vortex. The main steps of the phenomenon are understood, but especially concerning the inception and development of cavitation many unexplained details arise. Hence, a proper prediction of vortex cavitation inception is still difficult. Anyhow the basic principles of vortex generation can be summarized as follows. The pressure difference on suction and pressure side leads to a vortex at the hub and the tip of each propeller blade. Such a vortex in a viscous flow can be split into an inviscid outer region which behaves almost like a potential vortex and an inner viscous core. The velocity gradients inside the vortex lead to a reduction of pressure in the area of the vortex. The simplest model which describes such a flow is the so called Rankine vortex where the core is assumed to rotate like a rigid body. The tangential velocity and also the pressure can then be described as a function of radius. Here the non-dimensional radius r/R_c is chosen.

$$\begin{aligned} v_t(r) &= \frac{r}{R_c}\frac{\Gamma}{2\pi R_c} \qquad if: \quad r < R_c \\ &= \frac{\Gamma}{2\pi r} \quad else. \end{aligned} \tag{1}$$

$$\begin{aligned} c_p(r) &= -2 + \frac{r^2}{R_c^2} \qquad if: \quad r < R_c \\ &= -\frac{R_c^2}{r^2} \qquad else. \end{aligned} \tag{2}$$

and:

$$p_{vortex}(r) = p_\infty - c_p \frac{\rho}{2}\frac{\Gamma^2}{4\pi^2 R_c^2} \tag{3}$$

It is observed that real vortices do not reach the pressure minimum, which is predicted by the Rankine vortex model. A reason for this is the simplified assumption of a rigid rotating body inside the core. Among other more detailed models Hamel and Oseen derived a vortex formulation from the Navier-Stokes-Equation, see figure 1.

$$v_t(r) = \left(1 - e^{-\frac{r^2}{R_c^2}}\right)\frac{\Gamma}{2\pi r} \tag{4}$$

$$\begin{aligned} c_p(r) = &\left(1 - e^{-\frac{r^2}{R_c^2}}\right)\frac{R_c^2}{r^2} \\ &+2\left(Ei\left(-\frac{r^2}{R_c^2}\right) - Ei\left(-2\frac{r^2}{R_c^2}\right)\right) \end{aligned} \tag{5}$$

where Ei is the exponential integral.

Hamel and Oseen further derived a relation for the growth of a vortex core in a viscous fluid.

$$R_c^2 = 4\upsilon(t_0 + t) \tag{6}$$

In order to determine the pressure in the vortex its strength and the size of the core need to be known. The strength is related to the circulation generated by the blade and increases with the roll up process of the free vortices behind the blade. The size of the vortex core strongly depends on its history and especially its formation**.** McCormick, who derived a semi empiric method to estimate the effect of different Reynolds numbers on cavitation inception, could show that the thickness of the boundary layer affects the inception of cavitation. Following the assumptions of potential theory, where no boundary layer exists, it can be assumed that lift and circulation are almost independent of the boundary layer, for the propellers considered here. Hence, it can be concluded that the vortex core originates from the boundary layer of the blade [10], [1].

Fruman [3] related the core diameter, measured behind an elliptic wing to the thickness of the boundary layer at maximum chord. The size of the vortex core was measured with PIV-methods. The thickness is approximated according to a formula suggested by Schlichting, see [4] and [5]:

$$\delta = 0.37\, C\, \mathrm{Re}^{-0.2} \tag{7}$$

Szantyr [11] used the same relation for a similar model, but evaluated the equation at 0.95D/2. According to [6] a slightly different equation is used, which was derived for turbulent boundary layers, as turbulent layers are typical for full scale propellers.

$$\delta = 0.154\,\mathrm{Re}^{-\frac{1}{7}}\, C \tag{8}$$

The Reynolds number is the local Reynolds number at the tip while c is the chord length at the tip.

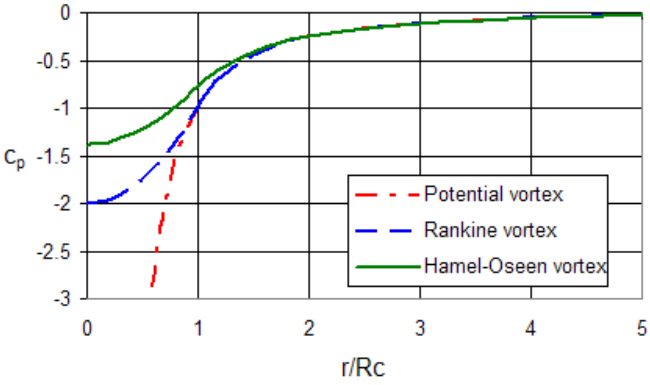

Figure 1: Radial pressure characteristic inside a vortex according to different vortex models.

The idea, which goes back to McCormick, to correlate the boundary layer thickness with the vortex core diameter generated by the tip vortex of a wing could be approved later on by several tests campaigns. But it has to be kept in mind, that it was not possible to extract a proper relationship between both values, which are independent from a special test setup.

A propeller typically generates two types of vortices in the trailing flow. At each blade a tip and a hub vortex are produced. While the tip vortex immediately sheds into the flow the hub vortex of a blade strongly interacts with the vortices of the other blades. The shape of the hub affects the further development of the hub vortex and also the local pressure level behind the propeller. For that reason only tip vortices are considered here.

Further uncertainties arise from the fact, that inception of vortex cavitation depends on the water quality, or more precisely on the number of nuclei in the water. It is reported, that this relation vanishes, if other types of cavitation, e. g. sheet or cloud cavitation, are already developed. Such detailed effects exceed the possibility of potential flow theory and will not be treated here.

BOUNDARY ELEMENT METHOD

Potential theory based methods are widely spread and known as reliable tools to calculate the flow around lifting and non-lifting bodies, as long as viscous effects can be almost neglected. This is also true for most propellers, especially if they operate in their design conditions. The method chosen to solve the described problem is a three dimensional boundary element method, where rectangular sources and doublets are distributed directly on the propeller surface with the collocation point in the middle.

The velocity potential, which is a solution of the continuity equation $\nabla\Phi = 0$, can be described as a sum of the undisturbed potential of the inflow and the induced potential of the propeller with its trailing free vortices.

$$\Phi(x) = -\frac{1}{4\pi}\left(\sum_{j=1}^{N_B}\sigma_j \int_{A_j}\frac{1}{r_j(x)}ds + \sum_{j=1}^{N_B+N_W}\mu_j \int_{A_j}\vec{n}_j\nabla\frac{1}{r_j(x)}ds\right) + \Phi_\infty \tag{9}$$

The induced potential can be split up into a source distribution on the blades to account for their displacement in the flow, and a doublet distribution on the body that extends as free vortices into the flow behind the propeller, which is mainly responsible for the generated lift. On the surface of the propeller a tangential flow boundary condition has to be fulfilled.

$$\vec{n}\,\vec{v} = 0 \tag{10}$$

This is formulated as a Neumann boundary condition, which allows a solution of the dipole strength distributed on the propeller. The strength of the sources is set to $\sigma = \vec{n}\vec{v}_{Panel}$, where $\vec{n}$ is the normal vector on the propeller pointing into the flow and $\vec{v}_{Panel}$ is the relative speed between a panel and the fluid at rest. At the trailing edge of a blade a Kutta condition can be applied so that the bound vorticity on the blade is able to shed into the trailing flow. The strength of these free vortices, which are called wake, is related to the dipole strength of the panels on the suction and pressure side at the trailing edge.

$$\mu_{Wake} = \mu_{upper} - \mu_{lower} \tag{11}$$

This wake structure is set up as a series of panels starting at the trailing edge which follows the streamlines of the flow. As the location of the streamlines is unknown at the beginning of the calculation it has to be calculated iteratively. For steady calculations an initial location of the wake structure has to be guessed by following the undisturbed flow. In a first iteration step the potential due to the propeller and the initial wake geometry are determined. As the wake field has to be free of forces, it must be aligned with the calculated potential. After the first iteration the velocity at the center of each wake panel is evaluated and the shape of the wake panels is distorted in the direction of the local flow. In steady cases this has to be done several times until the potential on the propeller converges. In unsteady cases the strength of the vorticity shed into the flow may vary with time. In such cases the wake structure is moved with the local velocities and a new panel is generated at the trailing edge, which fills the gap between the moved panels in the wake and the trailing edge.

The method is also able to handle unsteady inflows like ship wakes. A measured or calculated velocity distribution in a plane ahead of the propeller can be given to the solver. Though this velocity distribution usually cannot be described by a potential it is used as inflow to the propeller. It is treated to be constant in axial direction. This makes it possible to calculate the force amplitudes generated by the propeller in the inhomogeneous ship wake and allows a prediction where vortex cavitation develops.

If the potential generated by the propeller is known, the velocity and pressure distribution along the propeller blades can be calculated.

$$p - p_\infty = -\frac{\rho}{2}(v_\infty{}^2 - v^2) + \frac{\partial\Phi}{\partial t} \tag{12}$$

The produced thrust can be determined by summing up the pressure integrated over the panel surfaces. To obtain the torque, the lever arm of the panel center towards the rotation axis has to be multiplied with the force acting on the panel.

If potential theory is applied to solve a hydrodynamic problem, the influence of viscosity must be almost negligible. One of the most important limits in the application of potential theory is that no separation can be detected and that a free slip wall is assumed as boundary condition. This leads to the fact that no boundary layer develops and hence no friction forces can be calculated directly. Based on measurements and basic theoretical solutions coefficients have been derived which

relate the local Reynolds number on a flat plate to a frictional force. For each panel a local Reynolds number is determined by

$$\mathrm{Re} = \frac{v\, d_{LE}}{\upsilon}, \qquad (13)$$

where v is the relative speed between panel and flow, d_{LE} is the distance from the leading edge. Prandtl and Karman [6] proposed a friction resistance coefficient, which is valid for the turbulent boundary layer of a flat blade.

$$c_F = 0.059\,\mathrm{Re}^{-0.2} \qquad (14)$$

The coefficient is normalized by the fluid density and the local velocity. It is assumed, that the force acts into the direction of the velocity.

IMPLEMENTATION OF THE VORTEX CAVITATION MODEL

As discussed above, the pressure decrease in the tip vortex depends on the circulation which forms the vortex and the size of the core, where viscous effects play a significant role. The vortex strength is related to the bound circulation of the propeller blade. The iterative wake adaptation scheme leads to a roll up of the free vortices which shed from the trailing edge. The vortices leaving the tip of the blade form a helix which increases in size with the travelling distance away from the propeller. It is assumed that this helix can be replaced by an equivalent vortex of certain strength. Starting at the centre of the helix, which is defined by the outermost panels in the wake topology, the curvature of the helix decreases continuously. If the curvature between two neighbouring panels in the wake is too low, the contribution of the panels to the strength of the tip vortex is neglected. Instead of the curvature a common radius, which points into the middle of the helix, is determined based on the position of two adjacent panels. If this radius increases with a factor larger than 1.6 compared to the two previous adjacent panels, the strength of the latter panel does not contribute to the equivalent vortex.

This procedure can be applied for all panel stripes in the wake parallel to the trailing edge of a foil, each starting at the outermost panel originating from the blade tip. For each panel stripe a different vortex strength is obtained. For numerical reasons a few more criterions limit the extension of the equivalent vortex. If the direction of rotation of two neighbouring vortices changes, the strength of the outer vortex is determined. This can be the case for propeller designs with highly unloaded blade tips at high advance coefficients. To achieve a numerically stable result the strength of the equivalent vortex is averaged over several panel stripes.

The second factor that mainly influences the inception of cavitation is the size of the vortex core. Following the discussion above it can be related to the boundary layer thickness. The value δ is calculated using the local Reynolds number and the leading edge distance of the panels at the tip of the trailing edge. These are known from the frictional force acting on the panels. Hence, the thickness on pressure and suction side is estimated and 85% of the sum of both values is chosen to be the initial vortex core diameter. The value of 85% is achieved by correlating the calculated results to the measurements done by Boulon, et al. [2].

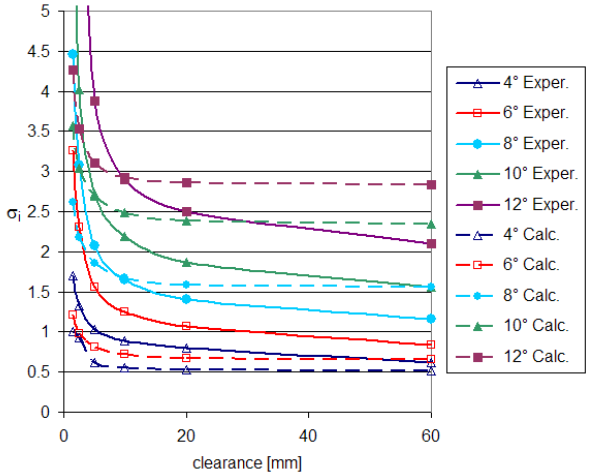

Figure 2: Cavitation inception number at different inclination angles and different clearance.

The size of the vortex core increases with the age of the vortex. According to the Hamel-Oseen vortex model the core radius grows with the square root of its age (6), which leads to an increment of $\sqrt{4\upsilon\Delta t}$ in unsteady calculations at each time step. In steady calculation the value Δt is related to the size of the panel.

The evaluation of the roll up process is always associated with the scheme the free vortices are moved after each iteration step. This is especially important at the outermost panels in the wake which originate from the tip. As the local flow velocity, which is the basis for the motion of the free vortices, cannot be evaluated at the edges of the panels itself, as the velocity potential is singular there. The velocity is evaluated at the panel centres instead and interpolated at the corners. This is not possible at the outermost panels and an adequate and stable extrapolation and smoothing has to be found. This influences the curvature of the wake directly and thus has an effect on the strength of the equivalent vortex.

RESULTS

As a first validation case the experimental setup published by Boulon et al. [2] have been used. In the test section of a cavitation tunnel a wing with elliptic shape has been mounted and the inception of cavitation has been detected. As an additional parameter a wall parallel to the main flow with an adjustable clearance to the tip has been installed. If the clearance is reduced, the load on the blade tip increases and hence vortex cavitation incepts earlier. The measurements have been performed at different inclination angles of the blade.

The cavitation number of inception is defined as:

$$\sigma_i = \frac{p_\infty - p_v}{\frac{\rho}{2} v_\infty^2} \qquad (15)$$

At the point of cavitation inception the pressure at the center of the vortex is equivalent to the vapor pressure.

$$p = p_v = p_\infty + p_{vortex}(r=0) \tag{16}$$

Using this equation the cavitation number of inception can directly be derived from the pressure inside the vortex:

$$\sigma_i = \frac{-p_{vortex}(r=0)}{\frac{\rho}{2} v_\infty^2} \tag{17}$$

Figure 2 shows the measured and calculated results of the vortex cavitation inception. The increasing cavitation number, which occurs with higher inclination angles, can be well predicted by the described model. At small inclination angles the predicted cavitation number is a bit too small, while at angles greater than 8° the cavitation is overestimated. The method also shows the dependency on the clearance, which is not as distinctive as observed in the measurement.

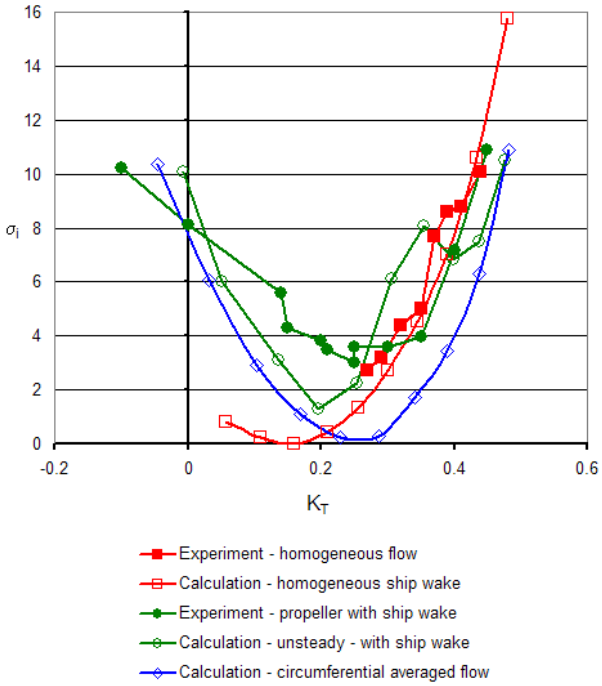

Figure 3: Cavitation inception of a marine propeller in homogeneous and inhomogeneous flow.

Aside from the complex hydrodynamic process, which cannot be fully modeled within such a basic method, different reasons can be expected for the deviations in the predicted cavitation number. The cavitation inception is measured at a point where the cavitating vortex is attached to the tip of the blade. The first cavitation inception in the vortex occurs at a σ, which is up to one unit higher than the number given in the measurements. At the given operation point where the cavitating vortex attaches to the blade two reasons for the cavity are possible. One is the reduced pressure in the vortex, another could be a local cavity, which originates from the low pressure at the leading edge and extends at the tip into the vortex. Though a few pictures are given by Boulon et al. it is not clear how the measured values have to be interpreted.

It seems that the influence of the wall close to the tip is underestimated. This might be due to the way of modeling the wall with sources distributed on the plane, where a free slip boundary condition is fulfilled. Probably the resolution of the wall was not sufficient to resolve the pressure gradients in this area. Another possibility would be to model a symmetry boundary condition at the position of the wall.

As a second validation case a marine propeller is chosen. For this propeller cavitation inception diagrams for homogeneous flow and also for the inhomogeneous flow behind a ship model were available, shown in figure 3.

The calculated values for the homogeneous flow correlate well with those measured. At $K_T = 0.15$ the tip is fully unloaded and almost no vortex leaves the tip. Hence the calculated cavitation number decreases to zero and in the experiment no cavitation, which can be clearly identified as vortex cavitation, occurs.

In the numerical analysis the wake generated by the ship can be treated in two ways. One approach is to implement the inhomogeneous wake field as inflow to the propeller, which requires an unsteady calculation. The alternative is to use circumferentially averaged velocities as inflow to the propeller. This allows a steady calculation where only one blade needs to be evaluated with respect to its periodic copies. The latter approach is much faster but does not reveal as much information as the unsteady approach.

Figure 3 shows that the cavitation bucket is shifted to higher K_T-values if the propeller operates in the wake field of the ship. The minimum of the calculated bucket using the circumferentially averaged inflow agrees with the measured one but its level is approximately two units too low. It has to be expected that the thrust values are shifted, because the axial velocity is decreased by the wake of the ship, which leads to a higher thrust. Also the underestimated cavitation inception using the averaged wake field can be explained. In regions, where the velocity in the wake is lower than the averaged velocity the loading of the propeller blade increases, which results into a temporarily higher vorticity shed into the flow.

If the full wake field is used cavitation incepts earlier, but it can be seen, that the inception curve does not have such a smooth characteristic as the other two calculated curves. The analysis of the free vortices is numerically much more difficult in the unsteady case, as intersections between the vortices may occur and lead to numerically instable results during their deformation between the time steps.

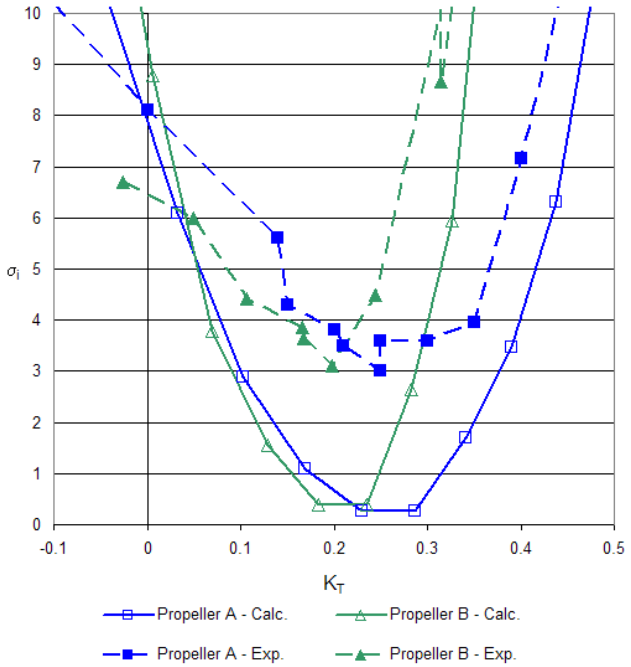

Figure 4: Comparison of the cavitation inception for two propellers measured behind a ship model and calculated using the circumferential averaged wake.

In figure 4 the cavitation performance of two propellers is compared. The measurements show that propeller A has a wider cavitation bucket than propeller B. Furthermore propeller A has a better performance at high load coefficients. Both properties are also predicted by the calculation. The pressure level at which cavitation occurs cannot be predicted if only a circumferentially averaged wake is used.

SCALE EFFECTS

Not only geometrical similarity and similar cavitation numbers have to be given to reproduce the same results but also Reynolds number has a strong influence on the vortex cavitation pattern. According to the work of McCormick a vortex cavitation inception behind a foil follows the rule:

$$\sigma_i = \alpha^n \, \mathrm{Re}^m \tag{18}$$

where α is the inclination angle of the foil and Re the characteristic Reynolds number.

Values for n and m are given in the literature and depend on the considered geometry and the flow regime (laminar or turbulent). Typical values are $n \approx 2$ while m is in the range between 0.3 and 0.4. If a propeller is scaled from model to full scale the inclination angle of the profile section remains almost the same, so that cavitation inception can be scaled with

$$(\mathrm{Re}_{Model} / \mathrm{Re}_{Full})^m . \tag{19}$$

As the pressure gradient inside the vortex is dominating the pressure level at the vortex the cavitation number of the propeller is set to:

$$\sigma_i = \frac{p_{\min}}{\frac{\rho}{2} n^2 D^2} = \frac{c_{p,\min} \frac{\rho \Gamma^2}{8\pi^2 R_c^2}}{\frac{\rho}{2} n^2 D^2} \tag{20}$$

The core diameter is estimated by an empiric formula for turbulent flows. Hence, the cavitation number can be extended to:

$$\begin{aligned} \sigma_i &= \frac{c_{p,\min} \rho \Gamma^2}{8\pi^2 (1.7 \cdot 0.154 \mathrm{Re}^{-\frac{1}{7}} C_{0.95D/2})^2 \frac{\rho}{2} n^2 D^2} \\ &= K_1 \left[\frac{\Gamma}{\mathrm{Re}^{-\frac{1}{7}} C_{0.95D/2} nD} \right]^2 \end{aligned} \tag{21}$$

It can be shown by dimensional analysis that the circulation Γ is proportional to $D^2 n$. Using this and regarding the fact that the chord length is always in a fixed relation to the diameter the influences on the cavitation number can be summarized to:

$$\sigma_i = K_2 \left[\frac{D^2 n}{\mathrm{Re}^{-\frac{1}{7}} DnD} \right]^2 = K_2 \, \mathrm{Re}^{\frac{2}{7}} \tag{22}$$

The derivation shows, that the developed method is in agreement with McCormick's rule and leads to the conclusion that a propeller scaled within the described method leads to a McCormick exponent of $m = \frac{2}{7} \approx 0.286$. This value is a bit smaller than those given in literature. As the value depends on the exponent used for the boundary layer model, it is difficult to compare it with the measured values, which have been derived from laminar or semi-turbulent tests.

The results presented here are all compared to model tests and hence the Reynolds number of the model was chosen in the calculation. As full scale results are difficult to measure, it is also difficult to select the correct McCormick exponent for the application; however a different exponent can be obtained if the boundary layer model, especially the exponent, is adjusted.

CONCLUSION

A model was developed to calculate the inception of vortex cavitation. It could be shown that despite many hydrodynamic simplifications, which had to be made, the cavitation performance of a propeller could be calculated. The strength of the tip vortex is determined by analysing the roll up process of the free vortices in the flow behind the propeller. The second term, which influences the inception of cavitation in the described model, is the boundary layer thickness. This is estimated by a formula validated for flat plates with a turbulent boundary layer. The model cannot account for small details of the geometry, which influence the formation of the vortex at the tip. Also an interaction with other developed cavities on the blade is not possible so far.

The proposed method is a quick and efficient way to predict vortex cavitation inception, as the computation time is almost negligible compared to the overall effort of a panel method. The alignment of the free vortices after each iteration

step and also the solution of the resulting system of linear equations require the major computation time. The roll up of the vortex in steady calculations needs at least three iteration steps until it is developed so far that a vortex cavitation prediction is possible. It has to be kept in mind that three iterations are also required to achieve a converged result regarding thrust and torque.

It can be concluded that the proposed method can be used to compare different propeller designs, like it is necessary in an automatic design process e. g. in an optimization loop. The width and also the position of the bucket can be used as suitable parameters. Nevertheless more validation work has to be done with different propeller types to obtain further information about the applicability of the method.

ACKNOWLEDGMENTS

We would like to thank ThyssenKrupp Marine Systems especially the shipyard HDW who supported this work.

NOMENCLATURE

A_j	area of the j-th panel
C	chord length
c_F	friction coefficient
c_p	pressure coefficient
d_{LE}	distance to the leading edge
ds	infinitesimal surface element of a panel
D	propeller diameter
Ei	exponential integral
K_T	thrust coefficient
$\vec{n}$	normal vector of a panel
n	rotation speed
N_B	number of panels on the body
N_W	number of panels in the free vortices conntected to the trailing edge
p	pressure
p_{vortex}	pressure inside the vortex
p_∞	reference pressure
r	radius inside the vortex
$r_j(x)$	distance between x and a point on the j-th panel
Re	characteristic Reynolds number
R_c	radius of the viscous vortex core
t	vortex age
t_0	initial vortex age
v	flow velocity
v_t	tangential velocity
v_∞	undisturbed flow velocity
x	location of the collocation point
α	inclination angle
Γ	circulation
δ	boundary layer thickness
Δt	time step
Φ	velocity potential
Φ_∞	undisturbed velocity potential
ρ	fluid density
σ_j	source strength of the j-th panel
σ_i	cavitation inception number
μ_j	dipole strength of the j-th panel
υ	cinematic viscosity

REFERENCES

[1] Arndt, E. A. 2002, "Cavitation in vortical flows", *Annual Review of Fluid*. Mech., 34, 143-175.

[2] Boulon, O., Callenaere, J.-P. F. and Michel, J.-M., 1999, "An experimental insight into the effect of confinement on tip vortex cavitation of an elliptical hydrofoil.", *J. of Fluid Mechanics*, 390, 1-23.

[3] Franc, J.-P. and Michel, J.-M., 2004, "Fundamentals of Cavitation", *Kluwer Acacdemic Publisher*.

[4] Fruman, D. H., 1995, "Effect of Hydrofoil Planform on Tip Vortex Roll-Up and Cavitation," *Transactions of the ASME.*. Vol 117, 192-169.

[5] Schlichting, H., 1979, Boundary Layer Theory, Sixth Edition, *McGraw-Hill, New York.*

[6] Hoerner, S. F., 1965, "Fluid-Dynamic Drag*", Bricktown N. J.*.

[7] Hsu, C.C, 1989, "Studies of scaling of tip vortex cavitation inception on marine lifting surfaces", *International Symposium on Cavitation Inception '89.*

[8] Latorre, R. et al., 1984, "Analysis of tip vortex cavitation inception from elliptical planform hydrofoils with roll-up and acoustic considerations", *International Symposium on Cavitation Inception '84*.

[9] Lee, H. and Kinnas, S. A., 2001, "Modelling of unsteady blade sheet and developed tip vortex cavitation.", *Fourth International Symposium on Cavitation*.

[10] McCormick, B. W., "On cavitation produced by a vortex trailing from a lifting surface", *J.Basic Eng*. 84:369–79.

[11] Szantyr, J. A., 2006, "A computational model of the propeller cavitation tip vortex interating with the rudder", *Sixth Inernational Symposium on Cavitation*.

[12] Truckenbrodt, E., 1999, „Fluidmechanik - Band 2: Elementare Strömungsvorgänge dichteveränderlicher Fluide sowie Potential- und Grenzschichtströmungen" *Springer Verlag Berlin Heidelberg*.